ACS SENSORS

pubs.acs.org/acssensors Article

Porous Silicon Fabry–Pérot Interferometer for *N*-Acetyl-*β*-D-Glucosaminidase Biomarker Monitoring

D. Nanda Kumar, Nofar Pinker, and Giorgi Shtenberg*

Cite This: https://dx.doi.org/10.1021/acssensors.0c00348 Read Online

ACCESS | Metrics & More | Article Recommendations | Supporting Information

ABSTRACT: Bovine mastitis (BM) is a prominent inflammatory disease affecting the dairy industry worldwide, originated by pathogenic agent invasion onto the mammary gland. Early detection of new BM cases is of high importance for infection control within the herd. Conventional analytical techniques lack the ability to detect BM-predicting biomarkers, used as analytical indicators for health status evaluation, in real time or outside the laboratory boundaries. Herein, we describe a biosensing platform for label-free detection and identification of BM onset through targeting *N*-acetyl-*β*-D-glucosaminidase (NAGase) for potential evidence-based therapy. The lysosomal activity in dissimilar milk qualities was monitored by a gelatin-functionalized porous Si Fabry–Pérot interferometer, while estimating the biochemical reaction precipitating products within the nanostructure. The optical response was proportional to the inherent NAGase concentration found in real milk samples, influenced by two dominant BM causative pathogens (i.e., *Escherichia coli* and *Streptococcus dysgalactiae*) at various somatic cell counts. Quantitative analysis of NAGase levels within the entire inflammatory spectrum (healthy, subclinical, and clinical BM) was obtained within the range of 1.0–4.2 μM/min (enzymatic activity per volume unit), while presenting a detection limit of 0.51 μM/min. The optical performances correspond with standardized biochemical activity assay in dissimilar milk qualities. Overall, the presented sensing concept exhibits the potential of BM-predicting biomarker detection using a simple and portable experimental setup for convenient early biodiagnostics and health status evaluation.

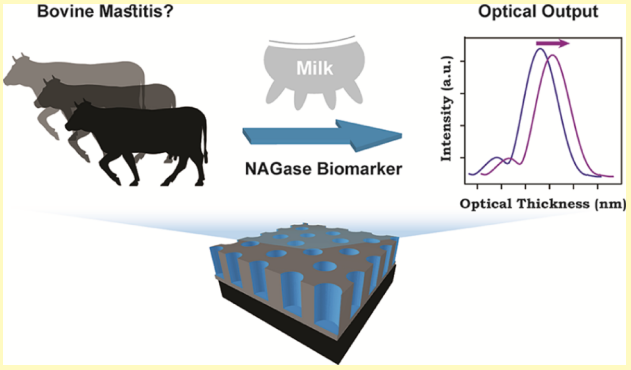

KEYWORDS: *bovine mastitis, NAGase, optical biosensor, pathogens, porous silicon, somatic cell counts*

Bovine mastitis (BM) is a prominent inflammatory disease affecting dairy industry worldwide, originated by pathogenic agent invasion onto the mammary gland.[1−3] Deteriorated clinical state correlates with reduced milk production, unsatisfying product quality, and augmented treatment costs.[4,5] BM can be categorized as chronic, clinical, and subclinical cases based on the severity of occurring inflammation.[2,6−8] Cows with clinical signs are easily recognized by abnormal milk (clots, flakes, and color change), irregular mammary glands (swelling and changes in tissue color), systemic illness, and are thus properly treated. In contrast, subclinical BM (>90% of the cases) are difficult to detect because of the absence of any visible indications.[1,2] Consequently, many of these cases remain undetected, leading not only to the spread of causative pathogens within the herd, but long-term untreated deteriorated health of the animal and hence a decline in the annual revenue.[4] Therefore, before BM becomes chronic, it is highly important to rapidly identify new BM cases for early infection control within the herd by antimicrobial therapy.[9,10] Conventional analytical approaches measure somatic cell counts (SCC), assess enzymatic activity, perform selective cell culture diagnosis, monitor electrical conductivity for on-line quality control, and even perform the California mastitis clotting test as a rapid cow-side examination.[4,8,11−13] Although some are very accurate, these methods lack the ability to detect BM-predicting biomarkers (e.g., haptoglobin, serum amyloid A, and *N*-acetyl-*β*-D-glucosaminidase—NAGase) in real time or outside the laboratory boundaries.[5,14] These biomarkers are used as predicting analytical indicators for health status evaluation, which vary their distribution in serum up to ∼100 folds upon inflammation or infection.[1,3,9,15,16] NAGase is a well-known BM biomarker, released upon damage or lysis of epithelial cells, therefore representing augmented impairment to the udder tissue.[1,7,17] The overall content of this intracellular lysosomal glycosidase is found to correlate with SCC,

Received: February 21, 2020
Accepted: June 23, 2020
Published: June 23, 2020

https://dx.doi.org/10.1021/acssensors.0c00348
ACS Sens. XXXX, XXX, XXX−XXX

differentiate BM pathogen types (major or minor), and thus can separate healthy quarters from all other inflamed statuses.[2,7,18] Among the various causative pathogens [e.g., *Staphylococcus aureus*, *Streptococci* (*uberis*, *dysgalactiae*, *agalactiae*)], *Escherichia coli* (*E. coli*) induces severe intramammary infection, usually resulting in clinical BM.[11,19] NAGase activity in untreated whole milk is performed by the fluorescence (FL)-based methodology developed by Kitchen et al.[18] Despite the known advantages of the procedure, for example, simple, rapid, affordable, and sensitive assessment of the emitted photons, it suffers from low-data availability that is obtained by expensive laboratory-based techniques. On the contrary, biosensors have a great potential to exceed these limitations and indeed, various biosensing schemes for BM biomarkers detection have demonstrated high sensitivity and selectivity and showed the potential to extrapolate the assay for on-site analysis.[3,5,9,10,12,20,21] Nirala and Shtenberg have modified the conventional NAGase activity assay by employing silica-coated zinc oxide quantum dots (6−8 nm) for enhanced FL.[16] Intensified emission values, over 11 fold, were achieved in correlation to SCC, pathogen type, and the severity of the occurring BM without hindering the optical performances.[16] Pemberton et al. have developed an unmodified screen-printed carbon electrode for amperometric analysis of NAGase activity by monitoring product oxidation.[17] The regenerative nature of the platform provides ample potential for continuous on-line or one-off disposable measurements of biological fluids. Despite the noted advantages of both feasibility concepts, these examples are still limited by at least one major constraint, expensive laboratory technique, or compatibility for whole milk analysis, which needs to be addressed in the next-generation biosensing design.

In the present work, we describe a label-free optical device for monitoring the biochemical activity of NAGase found in whole milk samples. The porous Si (PSi) Fabry−Pérot interferometer is a matured sensing and biosensing platform for diverse applications.[22−30] The versatility stems from several tunable features that are beneficial for biosensor's design. For example, the electrochemical anodization process can refine the physical properties of the nanostructure upon target's dimensions for optimized sensitivity and enhanced optical performance.[25,26] Moreover, the pores' external surface can be chemically and biologically decorated with capture probes according to the final sensing requirements or to minimize the matrix effects gained from interfering molecules.[22,25,31,32] The optical properties are effectively monitored using reflective interferometric Fourier transform spectroscopy (RIFTS), which is a highly sensitive technique for monitoring average refractive index alterations within the porous void.[22,23,30−38] Herein, the PSi nanostructure is applied for detection and identification of BM through evaluating the lysosomal activity of NAGase in different milk samples by spectral acquisition using a miniaturized portable platform. The biochemical reaction products precipitate and accumulate within the porous scaffold, thus altering the average refractive index, resulting in a shift of the optical position of the Fabry−Pérot fringe pattern.[23,31] The correlation between PSi optical response and NAGase activity was efficiently attained. The BM causative pathogens (*E. coli* and *S. dysgalactiae*) and SCC levels influence on the secreted NAGase content were evaluated with respect to the healthy udder. Finally, the optical performances were compared with the biochemical activity data of a conventional FL assay. Overall, our preliminary data exhibit the potential of the developed platform as a convenient biodiagnostic tool for BM detection while exceeding the constraints above.

EXPERIMENTAL SECTION

Materials. Boron-doped p^{++} silicon wafers (⟨100⟩ oriented with 0.9 mΩ cm resistivity) were supplied by Siltronix Silicon Technologies (France). Aqueous 48% hydrofluoric acid (HF), *N*,*N*-dimethylformamide (DMF), absolute ethanol (EtOH), and all analytical grade buffers were purchased from Merck Millipore (Israel). 3-Aminopropyltriethoxysilane (APTES), *N*,*N*-diisopropylethylamine (DIEA), *N*,*N*′-disuccinimidyl carbonate (DSC), acetonitrile, NAGase suspension from bovine kidney, 4-methylumbelliferyl-*N*-acetyl-β-D-glucosaminide (4-MUAG), gelatin, and 1-naphthol were obtained from Sigma-Aldrich Chemicals (Israel). Sodium nitrite, sodium hydroxide, 2-amino-2-methyl-1,3-propanediol, 3,3-dimethylglutaric acid, hydrochloric acid (HCl), and pararosaniline hydrochloride were supplied from Holland Moran (Israel). 1-Naphthyl-*N*-acetyl-β-D-glucosaminide was purchased from Apollo Scientific (Israel). 4-Methylumbelliferone (4-MU) was obtained from Alfa Aesar (Israel). Ultrapure water system (18.2 MΩ cm) from Thermo Fisher Scientific was used throughout the experiments.

Milk Sampling. Milk samples were obtained by authorized personnel from specific quarters of Holstein cows (Volcani Center research herd) and subjected to bacteriological tests, SCC, and NAGase assays.[15] Milk samples were classified as healthy, subclinical, and clinical mastitis, as previously described.[1,20,39] Animal experiments were approved by the Institutional Animal Care Committee of ARO, The Volcani Center (838/119IL).

NAGase Activity Pretreatment in Milk Samples. Milk samples were allowed to acclimatize to room temperature before homogenizing their content (×20 invert mixing). The hexazonium pararosaniline reagent was prepared as described by Kiernan.[40] First, 2 g of pararosaniline hydrochloride was dissolved in 16.6 mL HCl (2 N) and 83.4 mL ultrapure water followed by vigorous stirring overnight. The latter solution (1 mL) was mixed with 1 mL aqueous sodium nitrite (2% w/v) and 38 mL ultrapure water. Note: the resulting solution is stable up to 1 month at 4 °C. NAGase substrate solution was prepared by dissolving 10 mM of 1-naphthyl-*N*-acetyl-β-D-glucosaminide in 50 μL DMF followed by the addition of 450 μL 3,3-dimethylglutaric acidic buffer (pH 2.0). Equivalent volumes (500 μL) of milk and NAGase substrate solution were incubated for 1 h at 45 °C under continuous stirring to produce *N*-acetyl-β-D-glucosaminide and 1-naphthol reaction products.[17] Fixed concentrations of 1-naphthol (62.5, 125, 200, and 250 μM) were added to healthy milk and incubated similarly for acquiring the optical calibration curve. Finally, 500 μL of the mid-phase reaction mixture was mixed with 250 μL of hexazonium pararosaniline solution (pH 1.5) and 100 μL of 2-amino-2-methyl-1,3-propanediol (pH 10.5). Control experiments included the addition of the native NAGase suspension obtained from bovine kidney and thermally inactivated enzyme to eliminate any biochemical activity (3.7 units each). The suspensions were added to healthy milk samples and similarly pretreated.

Preparation and Biofunctionalization of Nanostructured PSi Transducers. PSi thin films were fabricated by electrochemical anodization, as previously described.[23,36] Briefly, a sacrificial layer (anodized by 375 mA cm^{-2} for 30 s in 3:1 v/v ratio of 48% HF and EtOH) was removed by alkaline dissolution (0.1 M sodium hydroxide) followed by mild postprocess polishing (1:1:3 v/v ratio of 48% HF, ultrapure water, and EtOH, respectively). Immediately, anodization of 525 mA cm^{-2} for 30 s was carried out. The freshly etched PSi nanostructures were thermally oxidized (800 °C for 1 h) under ambient conditions.[31] The resulting scaffold morphologies were characterized by Ultra Plus high-resolution scanning electron microscopy (HR-SEM, Carl Zeiss), operated at 1 kV. Next, the oxidized nanostructures (o-PSi) were amino-modified by APTES and DIEA (1% v/v, each) for DSC cross-linking (10 mM in acetonitrile), in accordance to our previous reports.[22,23,31] Gelatin solution (50 μL, 1% w/v) was applied on the DSC-modified surface for 30 min and

https://dx.doi.org/10.1021/acssensors.0c00348
ACS Sens. XXXX, XXX, XXX−XXX

rinsed thereafter to minimize nonspecific adsorption and to omit surface fouling by milk constituents (proteins, fat, sugars, and minerals). Finally, the surface was thoroughly rinsed with PBS buffer (pH 7.4) for 10 min three times and stored in a humidity chamber prior use.

Reflectivity-Based Evaluation NAGase Activity. Detailed description of the optical system setup and data analysis are described in Figure S1.[22,32,38] Briefly, reflectance spectra were collected using VIS-NIR Flame spectrometer Ocean Optics (FL, USA) in a wavelength range of 500−850 nm with a spectral acquisition of 80 ms saved every 30 s. The resulting data were analyzed using RIFTS as the effective optical thickness (EOT), proportional to the nanostructure average refractive index and the total depth governed by the Fabry−Pérot equation.[31,33] In the present work, the data are presented as the relative EOT

$$\text{Relative EOT} = \frac{\text{EOT}_{\text{milk sample}}}{\text{EOT}_0} \quad (1)$$

where $\text{EOT}_{\text{milk sample}}$ is the optical response following milk sample administration onto the porous nanostructure with respect to EOT_0 (averaged EOT values recorded during the initial optical experiment baseline). Gelatin-modified o-PSi surfaces were impregnated within a flow cell configuration and equilibrated by circulating PBS buffer (pH 7.4) for 10 min as an optical baseline. Then, the preincubated milk sample mixed with hexazonium pararosaniline solution and alkaline buffer were injected and allowed to react for 1 h. Lastly, the modified o-PSi was thoroughly washed with PBS buffer (pH 7.4) for 30 min to remove any unbound residues. The optical experiments were terminated once stable EOT values were obtained and performed under static conditions. Note: surface biofunctionalization was similarly characterized by measuring the relative EOT changes and evaluated by optical porosity using the spectroscopic liquid infiltration method (SLIM), as previously described.[22,33]

FL-Based Detection of NAGase Activity. The enzymatic assay was performed by a modified methodology proposed by Kitchen et al.[18] Briefly, 30 μL of milk and 40 μL of 4-MUAG (5 mM) in 0.25 M citrate buffer (pH 4.4) were pipetted into each microplate well. All reactions were allowed to react for 1 h at 45 °C followed by end-point FL examination (E_x/E_m of 354/460 nm) using a Varioskan LUX multimode microplate reader (Thermo Scientific). The obtained values were used to calculate NAGase activity using a standard calibration curve by assessing the FL of 4-MU (0−500 μM) in healthy milk samples.

RESULTS AND DISCUSSION

Optical Platform Design. The optical biosensing concept of NAGase biochemical reaction in the presence of specific substrate solution is illustrated in Scheme 1. 1-Naphthyl-*N*-acetyl-β-D-glucosaminide is hydrolyzed by NAGase present in the milk into *N*-acetyl-β-D-glucosaminide (nonreducing product) and 1-naphthol.[17] Sequentially, the latter product will react with hexazonium pararosaniline and will precipitate instantaneously.[40] The accumulated insoluble product (red color) within the porous nanostructure will modulate a noticeable change in the observed reflectivity spectrum that correlates with EOT values.[31] Overall, we have adapted azo coupling reaction of diazonium salts with 1-naphthol molecules to form strongly colored azo dye usually used in enzyme histochemistry, which are known for their insolubility (pH range 5−9).[40,41] Thus, the optical biosensing platforms for the detection of NAGase activity in the real milk samples were prescribed to accommodate sufficient enzymatic reaction products within the porous nanostructure.[23,33,36] The structural morphology of the resulting o-PSi single-layer platforms are shown in Figure S2, presenting cross-sectional and top-view HR-SEM images with an average pore size of 70 ± 15 nm

Scheme 1. Schematic Illustration of the o-PSi Optical Biosensor for Early Detection of BM through NAGase Activity Detection; a Miniaturized Platform Monitors the Precipitation of Biochemical Cascade Insoluble Products onto the Nanostructure Resulting in a Red Shift in the EOT; the Biochemical Cascade Includes NAGase Substrate Hydrolysis into *N*-Acetyl-β-D-glucosaminide and 1-Naphthol, in Which the Latter Reacts with Hexazonium Pararosaniline to Form an Insoluble Product

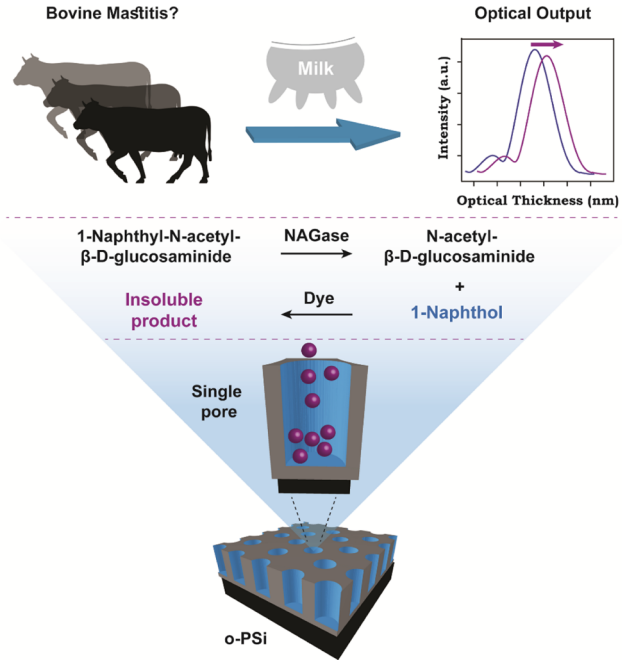

and ~8.3 μm thickness. Next, an important aspect while sensing a complex media as a real milk sample is the nonspecific adsorption of minute milk constituents within the porous scaffold and the influence of the fouling effect on the optical properties and its performances. Thus, gelatin solution (1% w/v), a widely used blocking agent in immunoblot assays, was applied onto the solid support through the conventional silanization technique to minimize the nanostructure fouling effect and to produce protein-resistant surface.[22,31,42,43] Gelatin attachment was confirmed by monitoring the relative EOT changes after each of the described biofunctionalization steps, which correspond to an increase in the average refractive index (Table S1).[22,25] Moreover, the bottom-up surface modification was assessed by SLIM, presenting a mild decrease in the optical porosity that represents the accessible volume within the nanostructure (Table S1). The optical performances of bare (unmodified) o-PSi and gelatin-modified surface with response to healthy milk samples were examined through RIFTS experiments. The optical experiments were designed to enclose o-PSi within a flow cell configuration and circulate PBS buffer (pH 7.4) until a stable optical baseline was obtained. Then, a healthy milk sample was introduced and incubated for 1 h, followed by vigorous buffer (PBS pH 7.4) rinsing procedure to remove any unbounded milk constituents. It is expected that the optical response of bare o-PSi toward milk constituents will result in a significant EOT change because of nonspecific binding.[32,34,35] In contrast, the gelatin-modified surface should repel and minimize nonspecific interactions of biological derivatives and nontarget molecules with the optical platform.[42] Indeed, bare o-PSi presents significant optical

https://dx.doi.org/10.1021/acssensors.0c00348
ACS Sens. XXXX, XXX, XXX−XXX

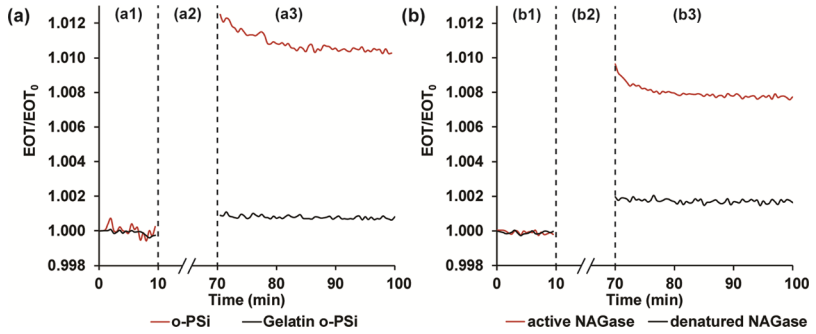

Figure 1. Relative EOT changes vs time of the different surfaces toward healthy milk samples. (a) Nonspecific adsorption estimation of bare o-PSi and gelatin-modified o-PSi with milk constituents. The optical transducer is first pretreated with PBS buffer (pH 7.4) to obtain baseline (a1), after which the milk sample is incubated for 1 h (a2), followed by buffer wash to remove any unbound and interfering residues within the milk (a3); (b) addition of the active and denatured NAGase suspension (3.7 units) onto the reaction solution (containing milk and 1-naphthyl-*N*-acetyl-*β*-D-glucosaminide). After the stable baseline (b1), a mixture of the reaction solution and the organic dye is injected and incubated for 1 h (b2), followed by a thorough buffer wash (b3). The optical signal is evaluated on gelatin-modified o-PSi.

response, whereas the gelatin-passivated surface depicts insignificant fouling of the nanostructure (values of 1.0101 and 1.0008 in the relative EOT, respectively); see Figure 1a. It should be mentioned that other blocking agents (e.g., BSA, caseins, myoglobin, skim milk, etc.) were studied, presenting poor protein resistance and elevated background noise (data not shown).

NAGase Activity in Simulated Conditions. Controlled conditions were used to examine the specific hydrolysis of 1-naphthyl-*N*-acetyl-*β*-D-glucosaminide into its products by the addition of the native NAGase suspension (3.7 units) onto the reaction solution.[7] A healthy milk sample was set as a control media, with insignificant SCC (71,000 cells/mL) and negative bacteriological signs, expecting minute NAGase activity. It should be highlighted that the final pH of the reaction solution, organic dye, and the alkaline buffer applied on the porous support result in pH 6.5, with insignificant implications on the structural stability of the biosensing platform.[33,44] Figure 1b depicts the optical response of NAGase-derived bovine kidney that was added onto the milk sample following the biochemical reaction cascade. Indeed, a significant increase in the relative EOT is obtained following the precipitation of the reaction products. This increase is a direct measure of NAGase specific biochemical reaction cascade, which eventually translates into insoluble product entrapment within the porous scaffold.[7] To further examine the specificity of the biochemical reaction, thermally denatured NAGase (inactivated enzyme) was similarly added onto the reaction solution and applied on gelatin-modified o-PSi. The optical response is minimized to 1.0016 in the relative EOT values because of mild enzymatic product infiltration onto o-PSi (Figure 1b). The latter is ascribed to the inherent NAGase content within a healthy milk sample, which activated the substrate hydrolysis cascade. The inherent content was verified through monitoring the optical response of a healthy milk sample without any enzymatic additives, presenting similar EOT values of 1.0018; see Figure S3. Additionally, the obtained EOT values are slightly higher than a control experiment performed in a healthy milk sample omitting the alkaline buffer from the protocol assay (Figure S3). The obtained net EOT shift between the latter two experiments strengthening the attributed optical signal is because of optimal precipitation conditions.

NAGase Activity within Different Milk Samples. The developed optical biosensing concept for lysosomal activity evaluation in correlation to BM severity was studied using real milk samples obtained from the Volcani Center research herd.[20] Table 1 presents the studied milk samples collected

Table 1. SCC and Bacteriological Contamination of Milk Samples

sample	SCC (×1000) cells/mL	pathogen
H	71	N/A
S1	353	*S. dysgalactiae*
S2	495	*S. dysgalactiae*
S3	>1000	*S. dysgalactiae*
E1	300	*E. coli*
E2	636	*E. coli*
E3	>1000	*E. coli*

from various udders, which represent the entire inflammation spectrum. Two major mastitis causative pathogens, *E. coli* and *S. dysgalactiae*, at different SCC levels (300−600 and >1000 × 10^3 cells/mL for subclinical and clinical mastitis, respectively) were evaluated by the optical setup. The healthy milk sample (H) was considered as a control condition, nondetected bacteriological findings and SCC <100 × 10^3 cells/mL, expecting insignificant lysosomal activity by the inherent NAGase content. All milk samples were subjected to similar pretreatment procedures and were later applied on gelatin-modified o-PSi to evaluate the relative EOT shift. Figure 2a depicts the reflective-based response of NAGase catalytic activity in different milk qualities, all positive with *S. dysgalactiae* pathogen. Significant increases in the relative EOT are attained proportionally to SCC level augmentation (1.0019, 1.0028, 1.0036, and 1.0051 for H, S1, S2, and S3, respectively). The optical signal represents the change in the average refractive index of the entire porous void because of infiltration and accumulation of the biochemical reaction products. Thus, increased mass transfer of the insoluble product within the nanostructure indicates the overall NAGase concentration and thus implies the severity of BM inflammation. Similar optical responses are obtained for *E. coli* pathogen contaminated milk samples (1.0024, 1.0045, and 1.0065 in the relative EOT for E1, E2, and E3, respectively) upon increased levels of SCC; see Figure 2b. These results strengthen the correlation between the optical biosensing output and NAGase lysosomal activity with respect to SCC growth. An additional control, sample blank, was used to estimate the background

https://dx.doi.org/10.1021/acssensors.0c00348
ACS Sens. XXXX, XXX, XXX−XXX

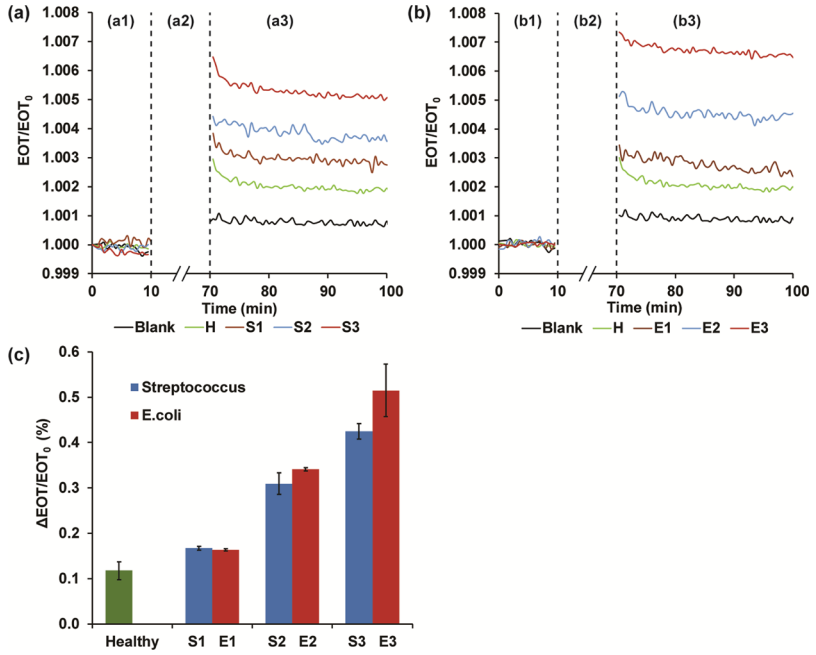

Figure 2. Reflective-based response of NAGase catalytic activity in various milk qualities. Representative relative EOT changes vs time of the gelatin-modified o-PSi throughout the optical experiment for milk samples positive to (a) *S. dysgalactiae* pathogen and (b) *E. coli* pathogen. After the stable baseline (a1,b1), a mixture of the reaction solution and dye is injected and incubated for 1 h (a2,b2), followed by a thorough buffer wash (a3,b3). (c) Averaged optical response after subtracting blank relative EOT value for the corresponding milk samples. Data are reported as mean ± SD ($n \geq 3$).

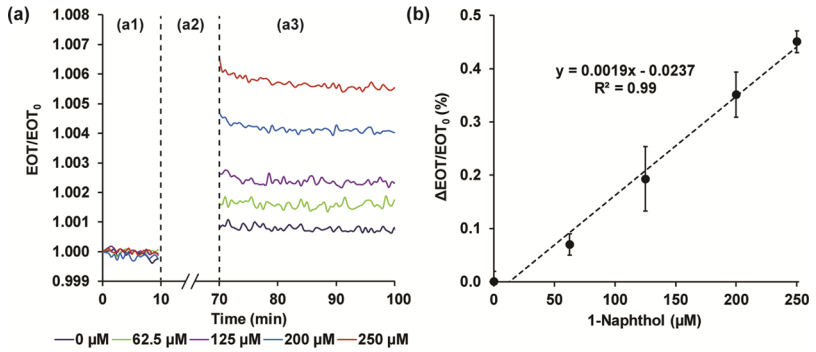

Figure 3. Biosensing system calibration with NAGase reaction product (1-naphthol). (a) Representative relative EOT changes vs time of the gelatin-modified o-PSi throughout the optical experiment for healthy milk samples spiked with known concentrations of 1-naphthol (0−250 μM). After the stable baseline (a1), a mixture of the reaction solution and dye is injected and incubated for 1 h (a2), followed by a thorough buffer wash (a3). (b) Calibration curve of the net optical response after subtracting the blank relative EOT value for the different 1-naphthol concentrations. Data are reported as mean ± SD ($n \geq 3$).

noise and the net response obtained from healthy milk (sample H) interaction with the porous support while omitted both the substrate solution and the pararosaniline dye from the bioassay, presenting an insignificant EOT shift of 1.0009 ± 0.0001. Figure 2c summarizes the corresponding net optical response in percentages ($\Delta EOT/EOT_0$) following subtracting blank relative EOT for the different milk samples at equivalent SCC values.[24,26] Both major BM-causing pathogens induce a profound increase in the net relative EOT for clinical mastitis (SCC >1000 × 10^3 cells/mL), where values of 0.51 ± 0.06 and 0.42 ± 0.02% are shown for E3 and S3, respectively. The elevated optical response is ascribed to the severity of the occurring BM at elevated SCC values, assuming higher NAGase activity.[7,15] The optical performances of *E. coli*-contaminated milk samples are higher than the induced response of *S. dysgalactiae* at equivalent SCC values (for all conditions >400 × 10^3 cells/mL), thus suspecting severe pathogenesis.[6,19] It should be highlighted that BM-causative pathogens have been previously linked to the animal's immune response severity, favoring *E. coli* over *S. dysgalactiae* as its inflammatory symptoms are severe at all stages of the disease.[20] Overall, the optical results correspond with our previous reports and others, linking an acute phase response because of animal's inflammatory state with augmented NAGase activity.[1,7,15,20] Moreover, the biosensing platform can efficiently differentiate between the various milk qualities in correlation to SCC values based on the substrate specific lysosomal activity.

NAGase Activity Quantification Based on RIFTS. The calibration curve for NAGase activity quantification was prepared using known concentrations of 1-naphthol (enzymatic reaction product) subjected to similar pretreatment

https://dx.doi.org/10.1021/acssensors.0c00348
ACS Sens. XXXX, XXX, XXX−XXX

conditions. Briefly, gelatin-modified o-PSi were immersed in PBS buffer (pH 7.4) for 10 min to acquire a stable baseline, followed by the preincubated solution of healthy milk samples, 1-naphthol (62.5, 150, 200, and 250 μM), and pararosaniline dye with an alkaline buffer for 1 h. Then, the nanostructure was thoroughly washed with PBS buffer to remove any unbound residues. Figure 3a depicts representative sensorgrams of the biosensing platform response toward different concentrations of 1-naphthol using RIFTS. The relative optical response is proportional to enzymatic reaction product concentration, in which higher insoluble products infiltrate within the nanostructure and induce a pronounced increase in the EOT. Figure 3b presents the calibration curve of the net optical response for standard 1-naphthol concentrations under the prescribed conditions. The linear trend of the reflectivity spectrum red-shifts in response to escalation of the 1-naphthol content and is governed by the fitted-regression equation of $\Delta EOT/EOT_0 = 0.0019 \times (C_{1\text{-naphthol}}) - 0.0237$ ($R^2 = 0.99$). From the obtained equation, the limit of detection was calculated as 31 μM (0.51 μM/min) using $3Sa/m$, where Sa is the standard of deviation and m is the slope of the linear portion.[23,25] The fitted-regression equation was used to calculate the enzymatic activity of NAGase in the studied milk samples based on RIFTS results (Table 2). The estimated

Table 2. NAGase Activity in Different Milk Samples Estimated by RIFTS and by the Conventional FL-Based Technique[a]

sample	RIFTS (μM/min)	FL assay (μM/min)
H	1.03 ± 0.18	1.41 ± 0.01
S1	1.46 ± 0.03	1.60 ± 0.07
S2	2.71 ± 0.21	2.72 ± 0.17
S3	3.73 ± 0.15	3.32 ± 0.04
E1	1.43 ± 0.02	1.96 ± 0.02
E2	2.99 ± 0.03	3.24 ± 0.18
E3	4.44 ± 0.50	4.00 ± 0.11

[a]Data are reported as mean ± SD ($n \geq 3$).

NAGase activity levels support the optical studies in which the lysosomal activity is increased with respect to SCC scores and the severity of the induced inflammation for both major pathogens. However, as previously mentioned, *E. coli* contamination induces severe pathogenesis to the mammary gland at progressed clinical stages. Thus, pronounced secretions of NAGase content onto milk were obtained for *E. coli* contamination over *S. dysgalactiae* while comparing corresponding SCC and health status (E2 and E3 over S2 and S3, respectively). Lastly, the obtained values from the optical inspection were affirmed by conventional FL assay. The latter is considered as a standard technique to evaluate NAGase activity within complex samples (i.e., milk and urine) and therefore deduce on animals' clinical health state.[16,18] The methodology includes nonfluorogenic substrate cleavage (4-MUAG) by NAGase into 4-MU, a fluorescent product. Figure S4 depicts the FL emission intensities of the analyzed milk samples, while the calibration curve of 4-MU (0−500 μM) spiked in healthy milk samples is presented in Figure S5. The calculated enzymatic activity levels of NAGase are summarized in Table 2. Similar trends are obtained for all analyzed milk samples considering SCC, the causative pathogen and the severity of BM, with respect to RIFTS results. The recovery values of the NAGase content quantified by the gelatin-modified porous nanostructure are within the range of 73−112%, which can be accredited to the sensitivity resolution of both sensing techniques. The conventional FL assay suppresses reflective-based methodology by assessing the emitted photons rather than the average refractive index of o-PSi, thus presenting a lower detection limit (0.66 and 31 μM, respectively). Despite the slight alteration of the absolute values by the biosensing platform, the overall trend is of importance for assessing animals' precise inflammatory status and therefore prescribing personal therapy treatment.[3,14] It should be mentioned that both RIFTS and FL assays cannot indicate on the specific bacterial specie causing the BM; therefore complementary microbiology examination should be involved.[7,10] Our experimental evidence played a crucial role for extrapolating the conventional NAGase assay for on-site detection using simple instrumentation (white light source and a miniaturized spectrometer). The efficiency of the optical concept and the rapid result availability cow-side can offer means for prompt BM severity diagnosis and imply on udder health status. Herdsman or veterinarian can utilize the optical indication for personalized treatment, meaning only those cows requiring attention will get it. The optical platform can also be adapted for BM recovery prognosis evaluation, producing an alternative means for conventional diagnosis practices. Overall, the developed label-free biosensing concept of monitoring NAGase activity levels by a passivated optical nanostructure is suitable for BM monitoring within real milk samples.

CONCLUSIONS

A variety of BM diagnostic tests are routinely used to evaluate the animal's health status based on inclusive parameters. Novel platforms for indicative biomarkers in milk detection are currently developed for early BM diagnosis and drug efficacy. In the present work, we describe a label-free optical device for monitoring the biochemical activity of NAGase found in whole milk samples using the RIFTS technique. The developed optical transducer can perform in real-life conditions (untreated milk, different SCC levels, and pathogens) and within the entire inflammatory spectrum (healthy, subclinical, and clinical BM). The presented sensing concept exhibits the potential of BM-predicting biomarker detection using a simple and portable experimental setup for convenient early biodiagnostics and health status evaluation. The methodology could be applied to study many other relevant composite systems with clinical implications by monitoring indicative biomarkers.

ASSOCIATED CONTENT

Supporting Information

The Supporting Information is available free of charge at https://pubs.acs.org/doi/10.1021/acssensors.0c00348.

Experimental setup used for the optical analysis; HR-SEM images; surface biofunctionalization characterization using RIFTS; optical characterization of healthy milk with and without alkaline buffer; FL emission intensities of the various milk samples for NAGase activity quantification; and FL assay calibration curve based on the 4-MU product within healthy milk samples (PDF)

https://dx.doi.org/10.1021/acssensors.0c00348
ACS Sens. XXXX, XXX, XXX−XXX

AUTHOR INFORMATION

Corresponding Author

Giorgi Shtenberg − *Institute of Agricultural Engineering, ARO, The Volcani Center, Bet Dagan 50250, Israel;* orcid.org/0000-0003-1234-1104; Phone: +972-50-7795925; Email: giorgi@agri.gov.il

Authors

D. Nanda Kumar − *Institute of Agricultural Engineering, ARO, The Volcani Center, Bet Dagan 50250, Israel*

Nofar Pinker − *Department of Biotechnology, Faculty of Agriculture, Food and Environment, The Hebrew University of Jerusalem, Rehovot 76100, Israel*

Complete contact information is available at: https://pubs.acs.org/10.1021/acssensors.0c00348

Notes

The authors declare no competing financial interest.

ACKNOWLEDGMENTS

This study was supported by the JCA Charitable Foundation (459-4610) and by The Israeli Chief Scientist of Ministry of Agriculture (20-07-0011), Israel.

REFERENCES

(1) Kalmus, P.; Simojoki, H.; Pyörälä, S.; Taponen, S.; Holopainen, J.; Orro, T. Milk haptoglobin, milk amyloid A, and N-acetyl-β-d-glucosaminidase activity in bovines with naturally occurring clinical mastitis diagnosed with a quantitative PCR test. *J. Dairy Sci.* **2013**, *96*, 3662−3670.

(2) Pyörälä, S.; Hovinen, M.; Simojoki, H.; Fitzpatrick, J.; Eckersall, P. D.; Orro, T. Acute phase proteins in milk in naturally acquired bovine mastitis caused by different pathogens. *Vet. Rec.* **2011**, *168*, 535.

(3) Viguier, C.; Arora, S.; Gilmartin, N.; Welbeck, K.; O'Kennedy, R. Mastitis detection: current trends and future perspectives. *Trends Biotechnol.* **2009**, *27*, 486−493.

(4) Seegers, H.; Fourichon, C.; Beaudeau, F. o. Production effects related to mastitis and mastitis economics in dairy cattle herds. *Vet. Res.* **2003**, *34*, 475−491.

(5) Mujawar, L. H.; Moers, A.; Norde, W.; van Amerongen, A. Rapid mastitis detection assay on porous nitrocellulose membrane slides. *Anal. Bioanal. Chem.* **2013**, *405*, 7469−7476.

(6) Blum, S. E.; Heller, E. D.; Jacoby, S.; Krifucks, O.; Leitner, G. Comparison of the immune responses associated with experimental bovine mastitis caused by different strains of Escherichia coli. *J. Dairy Res.* **2017**, *84*, 190−197.

(7) Hovinen, M.; Simojoki, H.; Pösö, R.; Suolaniemi, J.; Kalmus, P.; Suojala, L.; Pyörälä, S. N-acetyl-β-D-glucosaminidase activity in cow milk as an indicator of mastitis. *J. Dairy Res.* **2016**, *83*, 219−227.

(8) Koess, C.; Hamann, J. Detection of mastitis in the bovine mammary gland by flow cytometry at early stages. *J. Dairy Res.* **2008**, *75*, 225−232.

(9) Nirala, N. R.; Shtenberg, G. Gold Nanoparticle Size-Dependent Enhanced Chemiluminescence for Ultra-Sensitive Haptoglobin Biomarker Detection. *Biomolecules* **2019**, *9*, 372.

(10) Riffon, R.; Sayasith, K.; Khalil, H.; Dubreuil, P.; Drolet, M.; Lagacé, J. Development of a rapid and sensitive test for identification of major pathogens in bovine mastitis by PCR. *J. Clin. Microbiol.* **2001**, *39*, 2584−2589.

(11) Djabri, B.; Bareille, N.; Beaudeau, F. o.; Seegers, H. Quarter milk somatic cell count in infected dairy cows: a meta-analysis. *Vet. Res.* **2002**, *33*, 335−357.

(12) Chagunda, M. G. G.; Friggens, N. C.; Rasmussen, M. D.; Larsen, T. A model for detection of individual cow mastitis based on an indicator measured in milk. *J. Dairy Sci.* **2006**, *89*, 2980−2998.

(13) Singh, M.; Sharma, A.; Mittal, D.; Yadav, P.; Charaya, G. Assessment of lactate dehydrogenase enzyme activity in milk as a marker for detection of subclinical mastitis. *J. Anim. Res.* **2016**, *6*, 293.

(14) Ferrero, F. J.; Valledor, M.; Campo, J. C. Screening method for early detection of mastitis in cows. *Measurement* **2014**, *47*, 855−860.

(15) Nirala, N. R.; Pinker, N.; Desitti, C.; Shtenberg, G. Milk haptoglobin detection based on enhanced chemiluminescence of gold nanoparticles. *Talanta* **2019**, *197*, 257−263.

(16) Nirala, N. R.; Shtenberg, G. Enhanced fluorescence of N-acetyl-β-D-glucosaminidase activity by ZnO quantum dots for early stage mastitis evaluation. *Front. Chem.* **2019**, *7*, 754.

(17) Pemberton, R. M.; Hart, J. P.; Mottram, T. T. An assay for the enzyme N-acetyl-β-D-glucosaminidase (NAGase) based on electrochemical detection using screen-printed carbon electrodes (SPCEs). *Analyst* **2001**, *126*, 1866−1871.

(18) Kitchen, B. J.; Middleton, G.; Salmon, M. Bovine milk N-acetyl-β-D-glucosaminidase and its significance in the detection of abnormal udder secretions. *J. Dairy Res.* **1978**, *45*, 15−20.

(19) Burvenich, C.; Van Merris, V. r.; Mehrzad, J.; Diez-Fraile, A.; Duchateau, L. Severity of E. coli mastitis is mainly determined by cow factors. *Vet. Res.* **2003**, *34*, 521−564.

(20) Nirala, N. R.; Harel, Y.; Lellouche, J.-P.; Shtenberg, G. Ultrasensitive haptoglobin biomarker detection based on amplified chemiluminescence of magnetite nanoparticles. *J. Nanobiotechnol.* **2020**, *18*, 6.

(21) Wang, H.; Yuan, Y.; Zhuo, Y.; Chai, Y.; Yuan, R. Sensitive Electrochemiluminescence Immunosensor for Detection of N-Acetyl-β-d-glucosaminidase Based on a "Light-Switch" Molecule Combined with DNA Dendrimer. *Anal. Chem.* **2016**, *88*, 5797−5803.

(22) Massad-Ivanir, N.; Shtenberg, G.; Tzur, A.; Krepker, M. A.; Segal, E. Engineering Nanostructured Porous SiO_2 Surfaces for Bacteria Detection via "Direct Cell Capture". *Anal. Chem.* **2011**, *83*, 3282−3289.

(23) Shtenberg, G.; Massad-Ivanir, N.; Segal, E. Detection of trace heavy metal ions in water by nanostructured porous Si biosensors. *Analyst* **2015**, *140*, 4507−4514.

(24) Chhasatia, R.; Sweetman, M. J.; Prieto-Simon, B.; Voelcker, N. H. Performance optimisation of porous silicon rugate filter biosensor for the detection of insulin. *Sens. Actuators, B* **2018**, *273*, 1313−1322.

(25) Mariani, S.; Paghi, A.; La Mattina, A. A.; Debrassi, A.; Dähne, L.; Barillaro, G. Decoration of Porous Silicon with Gold Nanoparticles via Layer-by-Layer Nanoassembly for Interferometric and Hybrid Photonic/Plasmonic (Bio)sensing. *ACS Appl. Mater. Interfaces* **2019**, *11*, 43731−43740.

(26) Arshavsky-Graham, S.; Massad-Ivanir, N.; Segal, E.; Weiss, S. Porous silicon-based photonic biosensors: Current status and emerging applications. *Anal. Chem.* **2018**, *91*, 441−467.

(27) Jenie, S. N. A.; Plush, S. E.; Voelcker, N. H. Recent advances on luminescent enhancement-based porous silicon biosensors. *Pharm. Res.* **2016**, *33*, 2314−2336.

(28) Tieu, T.; Alba, M.; Elnathan, R.; Cifuentes-Rius, A.; Voelcker, N. H. Advances in porous silicon−based nanomaterials for diagnostic and therapeutic applications. *Adv. Ther.* **2019**, *2*, 1800095.

(29) Wang, J.; Sailor, M. J.; Chang, B. Y. Fabrication of a Lateral Gradient Rugate in Porous Silicon for a Miniature Spectrometer Application. *ChemElectroChem* **2019**, *6*, 5967−5972.

(30) Cheng, X.; Guan, B. Optical Biosensing and Bioimaging with Porous Silicon and Silicon Quantum Dots (Invited Review). *Prog. Electromagn. Res.* **2017**, *160*, 103−121.

(31) Shtenberg, G.; Massad-Ivanir, N.; Fruk, L.; Segal, E. Nanostructured porous Si optical biosensors: effect of thermal oxidation on their performance and properties. *ACS Appl. Mater. Interfaces* **2014**, *6*, 16049−16055.

(32) Schwartz, M. P.; Alvarez, S. D.; Sailor, M. J. Porous SiO_2 interferometric biosensor for quantitative determination of protein interactions: binding of protein A to immunoglobulins derived from different species. *Anal. Chem.* **2007**, *79*, 327−334.

(33) Sailor, M. J. *Porous Silicon in Practice: Preparation, Characterization and Applications*; John Wiley & Sons: Weinheim, Germany, 2012.
(34) Sweetman, M. J.; Harding, F. J.; Graney, S. D.; Voelcker, N. H. Effect of oligoethylene glycol moieties in porous silicon surface functionalisation on protein adsorption and cell attachment. *Appl. Surf. Sci.* **2011**, *257*, 6768−6774.
(35) Joung, C.-K.; Kim, H.-N.; Lim, M.-C.; Jeon, T.-J.; Kim, H.-Y.; Kim, Y.-R. A nanoporous membrane-based impedimetric immunosensor for label-free detection of pathogenic bacteria in whole milk. *Biosens. Bioelectron.* **2013**, *44*, 210−215.
(36) Shtenberg, G.; Massad-Ivanir, N.; Engin, S.; Sharon, M.; Fruk, L.; Segal, E. DNA-directed immobilization of horseradish peroxidase onto porous SiO_2 optical transducers. *Nanoscale Res. Lett.* **2012**, *7*, 443.
(37) Lin, V. S.; Motesharei, K.; Dancil, K.-P. S.; Sailor, M. J.; Ghadiri, M. R. A porous silicon-based optical interferometric biosensor. *Science* **1997**, *278*, 840−843.
(38) Janshoff, A.; Dancil, K.-P. S.; Steinem, C.; Greiner, D. P.; Lin, V. S.-Y.; Gurtner, C.; Motesharei, K.; Sailor, M. J.; Ghadiri, M. R. Macroporous p-Type silicon Fabry−Perot layers. Fabrication, characterization, and applications in biosensing. *J. Am. Chem. Soc.* **1998**, *120*, 12108−12116.
(39) Martins, S. A. M.; Martins, V. C.; Cardoso, F. A.; Germano, J.; Rodrigues, M.; Duarte, C.; Bexiga, R.; Cardoso, S.; Freitas, P. P. Biosensors for On-Farm Diagnosis of Mastitis. *Front. Bioeng. Biotech.* **2019**, *7*, 186.
(40) Kiernan, J. Hexazonium pararosaniline as a fixative for animal tissues. *Biotech. Histochem.* **2004**, *79*, 203−210.
(41) Menten, M. L.; Junge, J.; Green, M. H. A coupling histochemical azo dye test for alkaline phosphatase in the kidney. *J. Biol. Chem.* **1944**, *153*, 471−477.
(42) Craig, W. Y.; Poulin, S. E.; Collins, M. F.; Ledue, T. B.; Ritchie, R. F. Background staining in immunoblot assays reduction of signal caused by cross-reactivity with blocking agents. *J. Immunol. Methods* **1993**, *158*, 67−76.
(43) Terracciano, M.; Rea, I.; Politi, J.; De Stefano, L. Optical characterization of aminosilane-modified silicon dioxide surface for biosensing. *J. Eur. Opt. Soc.* **2013**, *8*, 13075.
(44) Sailor, M. J. Chemical Reactivity and Surface Chemistry of Porous Silicon. *Handbook of Porous Silicon*; Springer, 2014; pp 355−380.

https://dx.doi.org/10.1021/acssensors.0c00348
ACS Sens. XXXX, XXX, XXX−XXX